

PHASE TRANSITION OF NANOPARTICLES OF ORGANIC PIGMENTS

Masaki Kakuichi, Kazuo Kasatani*, Yuki Morita

*Graduate School of Science and Engineering, Yamaguchi University
Ube 755-8611, Japan*

*(*Corresponding author: kasatani@yamaguchi-u.ac.jp)*

ABSTRACT

Phase transition of nanoparticles of organic pigments was studied. Conditions under which phase transition of nanoparticles occurs were optimized. N-methylpyrrolidone solution of 3,6-diphenyl-2,5-dihydropyrrolo[3,4-c]pyrrole-1,4-dione (DPP), a derivative of diketopyrrolopyrrole, was diluted in vigorously stirred aqueous ethanol solution. Colloidal solution was then obtained. This solution was annealed at 60°C. UV/visible absorption spectra of DPP nanoparticles show that the wavelength of main absorption band shifted from 530 nm to 545 nm after annealing, the absorbance of the band increased, and sharpening of the main band was also observed. From these results, it was suggested that the phase transition to J-like aggregates occurred by annealing. Phase transition of nanoparticles of violanthrone 79 was also observed.

KEYWORDS: Nanoparticle, Diketopyrrolopyrrole derivative, Violanthrone 79, UV/visible absorption spectrum

1. INTRODUCTION

Nanoparticles are particles having a size range from 1 nm to several hundred nm. Physical properties of nanoparticles are different from those of bulk crystals, atoms, and molecules. For example, if particles are smaller than tens of nanometers, phenomena such as quantum size effect (Cini et al.) and quantum confinement effect (Takagahara et al.) can be observed. The practical applications of nanoparticles are optical materials (Kelly et al.), catalyses (Crooks et al.), and medical materials (Ito et al.). While nanoparticles of inorganic semiconductors have a lot of practical application, organic nanoparticles have not yet been used widely. Since organic compounds have huge variety, we can expect wide practical application of organic nanoparticles. For example, the use of organic nanoparticles rather than inorganic nanoparticles can be expected to reduce the invasiveness of the human body in the medical field.

Preparation of organic nanoparticles is classified to the build-up method and top-down method. Examples of the former are a mechanical grinding method and a method of laser ablation in a liquid (Tamaki et al., 2000, 2002, 2003, Mafune et al., Tsuji et al.), and those of the latter are a reprecipitation method (Kasai et al., 1992, 1995, 1996, Katagi et al., Tan et al., Fu et al.) and chemical synthesis. The reprecipitation method is a method to fabricate nanoparticles, in which a material is dissolved in a good solvent and the solution is diluted in a stirred poor solvent drop wise. The reprecipitation method is convenient and easy to modify; properties of nanoparticles, such as, particle size (Tan et al., Fu et al., Al-Kaysi et al.), size distribution, morphology (Al-Kaysi et al.) melting point, crystallinity, etc. can be changed.

In a previous paper, we reported phase transition of nanoparticles of violanthrone 78 (V78) (Kakuichi et al.). Nanoparticles of V78 were made by a reprecipitation method using aqueous ethanol as a poor

solvent, and then the nanoparticles were annealed to obtain J-like aggregate. Temperature of annealing was as low as 60°C.

In the present study, adding ethanol to the poor solvent and heating the nanoparticles made by reprecipitation method, we have obtained DPP nanoparticles with properties of J-like aggregates. We think this is a kind of phase transition. In the present paper, we report details of fabrication and the properties of the J-like aggregate nanoparticles of DPP. Phase transition of nanoparticles of V79 was also observed.

2. EXPERIMENTAL

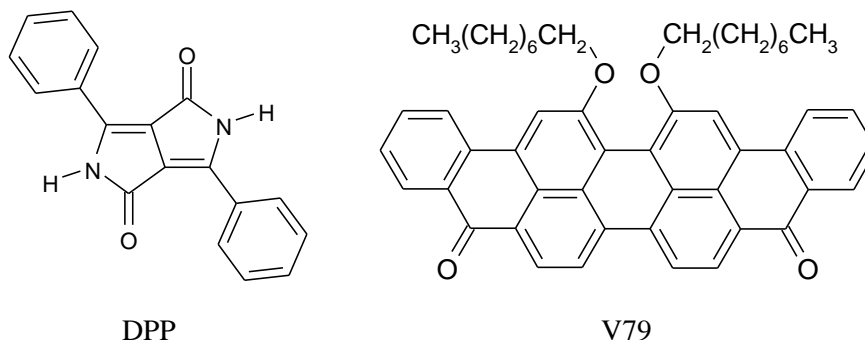


Figure 1: Structural formulas of organic pigments used.

Figure 1 shows structural formulas of organic pigments used. DPP was purchased from Tokyo Chemical Industry Co. and used without further purification. V79 was purchased from Aldrich Co. and used without further purification.

Typical condition for preparing nanoparticles of DPP was as follows: about 0.2 ml of N-methylpyrrolidone (NMP) solution of DPP (ca. 1.0×10^{-3} M) was injected using a microsyringe into 10 ml of vigorously stirred aqueous ethanol at 5°C. The obtained nanoparticles were filtrated with membrane filter of 800 nm pore size, and the filtrate was annealed at 60°C for at least 2 hours.

Typical condition for preparing nanoparticles of V79 was as follows: about 0.2 ml of tetrahydrofuran (THF) solution of V79 (ca. 1.0×10^{-3} M) was injected using a microsyringe into 10 ml of vigorously stirred aqueous acetone at room temperature. The obtained nanoparticles were filtrated with a paper filter, and the filtrate was annealed at 60°C for at least 15 hours.

UV/visible spectra were measured with a JASCO spectrometer V-550.

3. RESULTS AND DISCUSSION

We optimized fabrication conditions for DPP nanoparticles of J-like aggregates. The optimized conditions were concentration of DPP in good solvent, amount of the DPP solution, drip rate, composition of the poor solvent, temperature of poor solvent, stirring rate, annealing temperature, and annealing time.

Figure 2 shows UV/visible spectra of DPP nanoparticles together with a spectrum of NMP solution of DPP. The light blue line shows the spectrum of nanoparticles made under optimized conditions. The blue line shows that of the same nanoparticles before annealing. Annealing made the main band sharper and shifted from 530 nm to 545 nm. A sharp and red-shifted band is a characteristic of J aggregates. However, the sharpness of the main band does not look sufficient to describe the particles as J aggregates; we describe the nanoparticles as J-like aggregates.

We were unable to obtain J-like aggregates of DPP at any annealing temperature when we used pure water as a poor solvent. We also used pure ethanol as a poor solvent, but only large microparticles were obtained. Finally we found that a mixture of water and ethanol was suitable to obtain nanoparticles of DPP with J-like characteristics. We believe ethanol molecules are included in a nanoparticle, and ethanol molecules work as a lubricant in a nanoparticle upon phase transition.

Figure 3 shows the dependence of UV/visible absorption spectra of DPP nanoparticles on the composition of the poor solvent. The other experimental conditions were optimized ones. The best ethanol concentration of the poor solvent was 25 vol%.

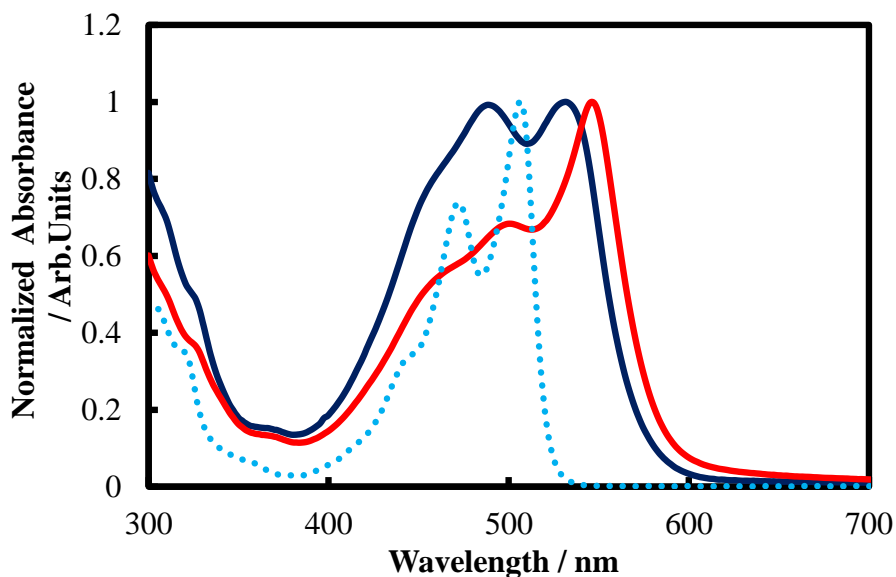


Figure 2: UV/visible absorption spectra of DPP nanoparticles with (red solid line) and without (dark blue solid line) annealing. Spectrum of DPP in an NMP solution (light blue dotted line) is also shown.

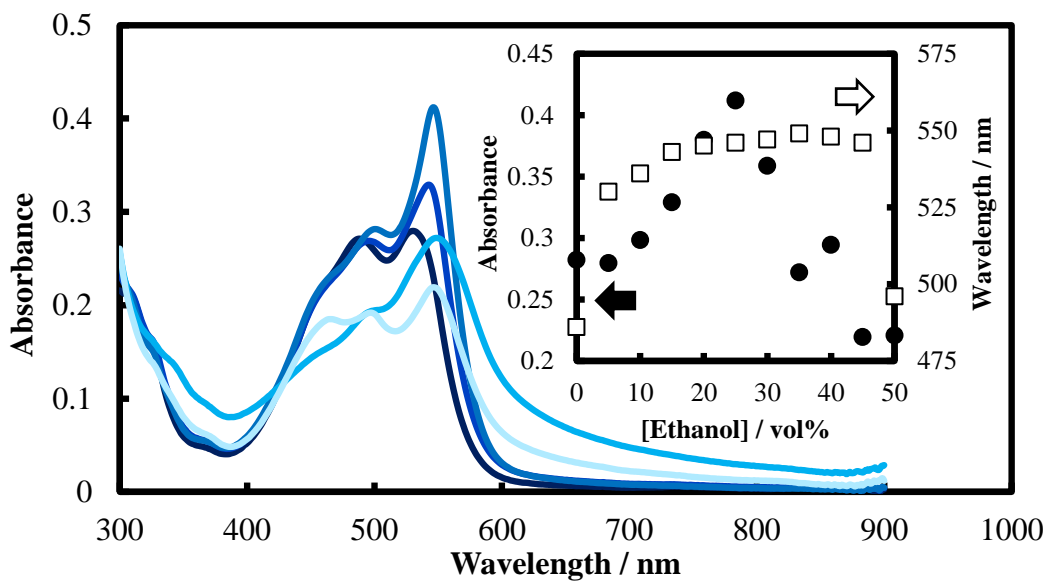


Figure 3: Dependence of UV/visible absorption spectra of DPP nanoparticles on the ethanol concentration of the poor solvent. The ethanol concentration was in a range from 5 vol% (the darkest blue line) to 45 vol% (the lightest blue line). The inserted figure is a plot of maximum absorbance and wavelength of maximum absorption vs. ethanol concentration.

Figure 4 shows the dependence of UV/visible absorption spectra of DPP nanoparticles on annealing temperature. The other experimental conditions were optimized ones. The dependence was rather critical; 60°C was the best annealing temperature. UV/visible absorption spectrum of nanoparticles annealed at 70°C has a broad band which was often observed for microparticles. We think that aggregation at a high

temperature is the cause of the broad band. Though we observed phase transition of DPP nanoparticles at as low as 60°C, generally phase transition of organic crystals needed much higher temperature than nanoparticles. For example, the single crystals of 2,3-bis(phenylethenyl)-5,6-dicyanopyrazine underwent a morphological phase transformation from a yellow crystal to an orange one via a thermal phase transition without the crystal state collapsing. The transformation began at a single starting point in the yellow crystal and then spread out into the whole crystal like a domino at 174.5°C (Ahn et al.). We expected that phase transition of organic crystals in small size, i.e. in nanoparticles, can occur much more easily.

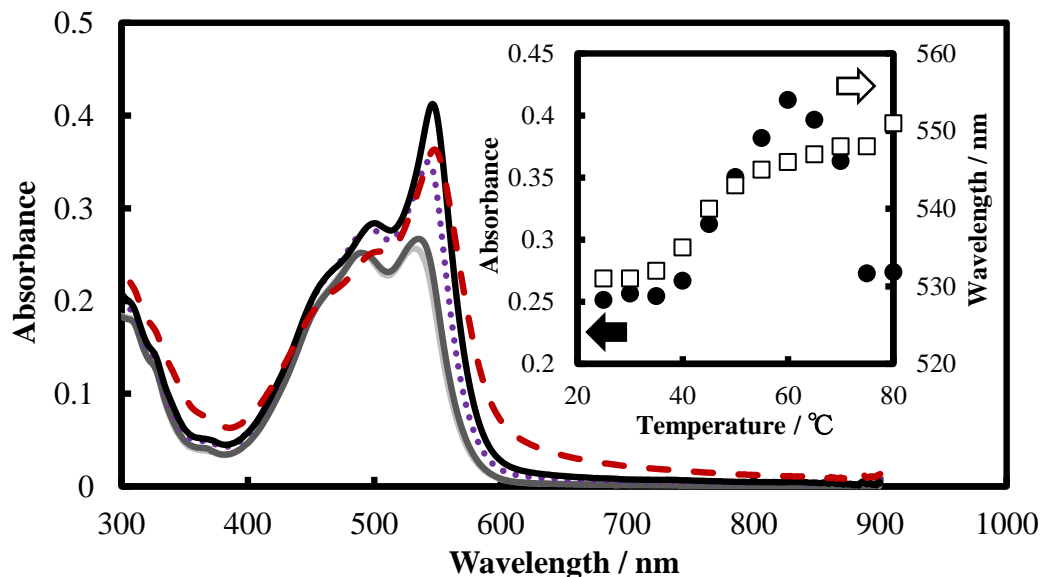


Figure 4: Dependence of UV/visible absorption spectra of DPP nanoparticles on annealing temperature. Annealing temperature is 50°C (light gray solid line), 55°C (dark gray solid line), 60°C (black solid line), 65°C (purple dotted line), and 70°C (dark red broken line).

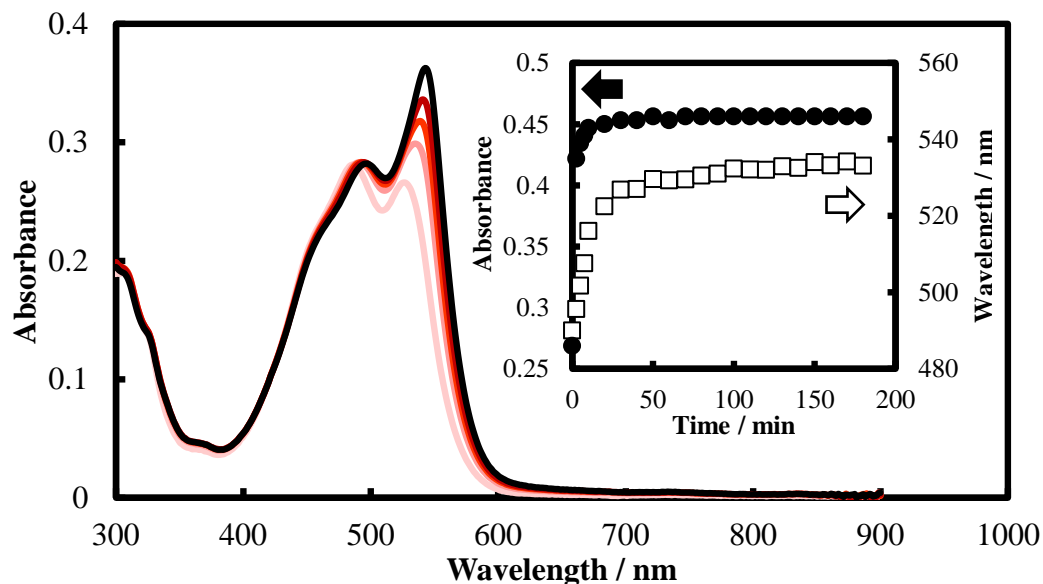


Figure 5: Dependence of UV/visible absorption spectra of DPP nanoparticles on annealing time. Annealing time is in a range from 0 minute (the lightest red line) to 10 minutes (the black line). The increment is 2.5 minutes. The inserted figure is a plot of maximum absorbance and wavelength of maximum absorption vs. annealing time.

Figure 5 shows the dependence of UV/visible absorption spectra of DPP nanoparticles on annealing time. The other experimental conditions were optimized ones. Annealing time must longer than 0.5 hours, and 2 or 3 hours are desirable.

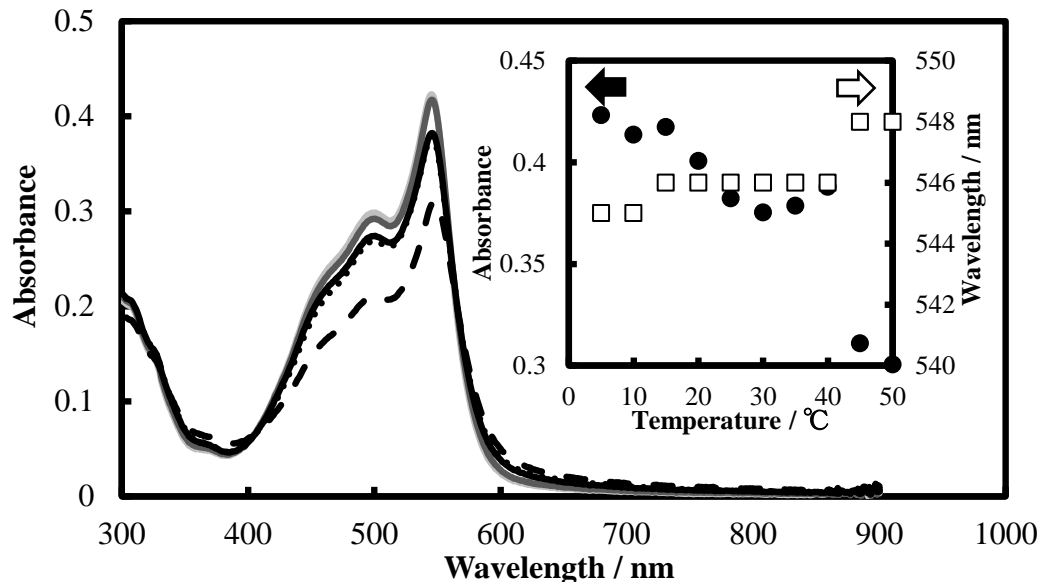


Figure 6: Dependence of UV/visible absorption spectra of DPP nanoparticles on temperature of the poor solvent. Temperature of the poor solvent is 10°C (light gray solid line), 20°C (dark gray solid line), 30°C (black solid line), 40°C (black dotted line), and 50°C (black broken line).

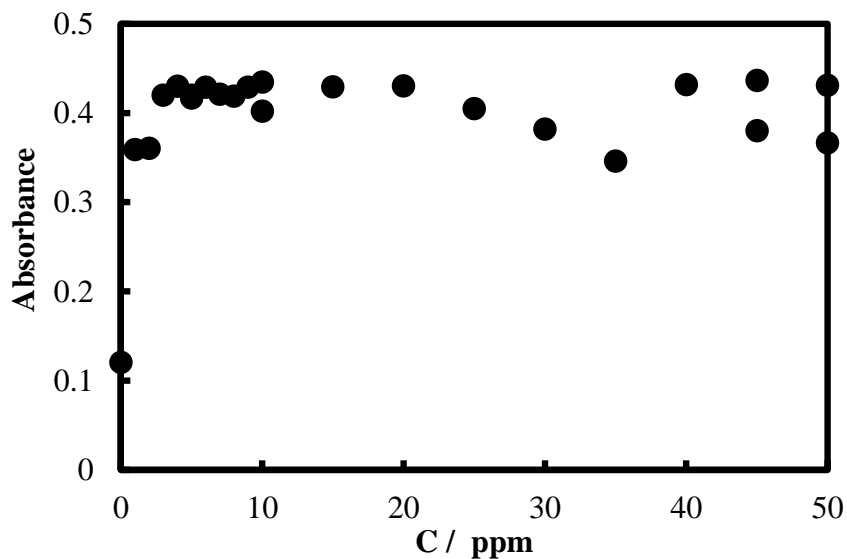


Figure 7: Dependence of absorbance of DPP nanoparticles of J-like aggregates on poly(vinyl alcohol) concentration in the poor solvent.

Figure 6 shows the dependence of UV/visible absorption spectra of DPP nanoparticles on the temperature of the poor solvent in which a solution of DPP was diluted. The other experimental conditions were optimized ones. First, we thought if we diluted DPP solution in the poor solvent at 60°C, annealing process might not be necessary. However, the best temperature range for the poor solvent was from 5°C to 15°C. Nanoparticles made at high temperature in the poor solvent may be in great disorder and it is a little difficult to change them to J-like aggregates upon annealing.

In a previous paper, we reported that addition of poly(vinyl alcohol) (PVA) even at concentration as low as 1 ppm in water as a poor solvent improved production of anthracene nanoparticles drastically (Kasatani et al.) . We only obtained anthracene microparticles instead of nanoparticles without PVA. This time we studied the effect of addition of PVA to the poor solvent for DPP nanoparticles.

Figure 7 shows the results; absorption spectrum of DPP nanoparticles made without PVA shows very low absorbance, which means existence of few particles. Addition of PVA into water at a concentration of as low as 1 ppm drastically improved nanoparticle formation.

We also changed stirring rate of poor solvent. Final concentration of J-like aggregate nanoparticles increased with stirring rate, but this effect was very limited.

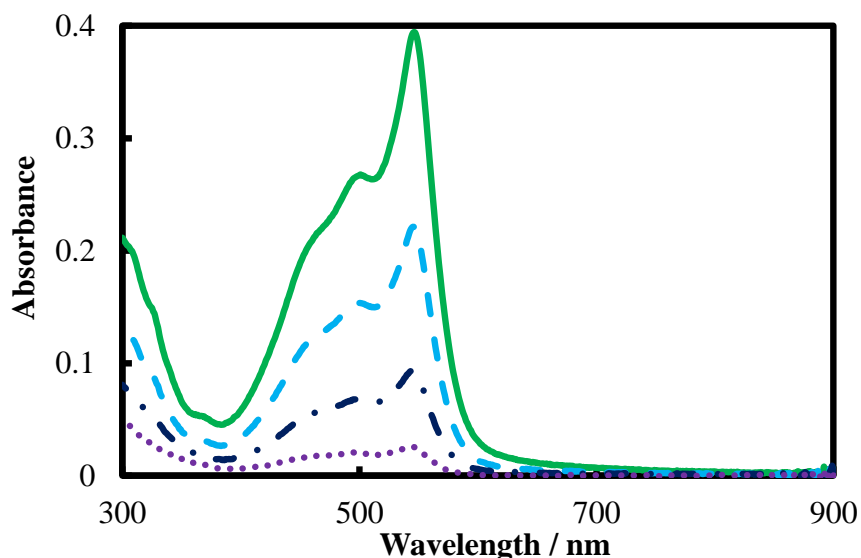


Figure 8: UV/visible absorption spectra of DPP J-like aggregate nanoparticles after filtration with membrane filters of specified pore size. Pore size was 800 nm (green solid line), 450 nm (light blue broken line), 300 nm (blue dot-and-dash line), and 200 nm (purple dotted line)

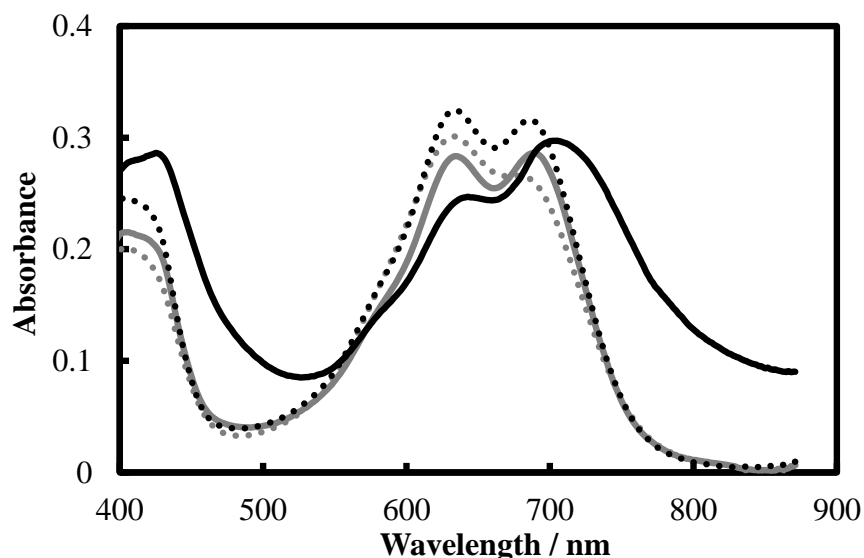


Figure 9: Dependence of UV/visible absorption spectra of V79 nanoparticles on the concentration of the poor solvent. Etanol:Water = 35:65 (gray lines), Acetone:Water = 50:50 (black lines). V79 nanoparticles with (solid lines) and without (dotted lines) annealing. Annealing time is 17 h, 22 h respectively. Temperature of annealing: 60°C

The diameter distribution of the J-like aggregate nanoparticles was estimated by measuring UV/visible absorption spectra after filtration with membrane filters. Figure 8 shows the results; most particles have diameters in a range from 300 nm to 450 nm.

Figure 9 shows the dependence of UV/visible absorption spectra of V79 nanoparticles on the composition of the poor solvent. Phase transition of V79 did not occur in water. Also, phase transition of V79 nanoparticles did not occur in aqueous ethanol. Only the phase transition of V79 nanoparticles occurred in aqueous acetone. The best acetone concentration of the poor solvent was acetone:water = 50:50. The best annealing temperature was 60°C, and the annealing time should be longer than 15 hours. The best temperature of the poor solvent was 25°C. However, the UV/visible absorption band of V79 J-like aggregates was a little broad.

4. CONCLUSIONS

Phase transition of DPP nanoparticles to J-like aggregates was observed. Nanoparticles of DPP were made by a reprecipitation method using aqueous ethanol as a poor solvent, and then the nanoparticles were annealed to obtain J-like aggregates. The fabrication conditions for J-like aggregate nanoparticles of DPP were optimized as follows:

Ethanol concentration of poor solvent: 25 vol%

Annealing temperature: 60°C

Annealing time: longer than 0.5 hours

Temperature of the poor solvent: 5°C

The fabrication conditions for J-like aggregate nanoparticles of V79 were optimized as follows:

Acetone concentration of poor solvent: 50 vol%

Annealing temperature: 60°C

Annealing time: longer than 15 hours

Temperature of the poor solvent: 25°C

5. REFERENCES

- Ahn, K.S. et al. (2011) Domino-like Thermal Phase Transition of 2,3-Bis(phenylethenyl)-5,6-dicyanopyrazine Crystal. *Dyes and Pigments*, 89, 93-95.
- Al-Kaysi, R. O. et al. (2005) Effects of Sonication on the Size and Crystallinity of Stable Zwitterionic Organic Nanoparticles Formed by Reprecipitation in Water. *Langmuir*, 21, 7990-7994.
- Cini, M. and Ascarelli, P., (1974) Quantum Size Effects in Metal Particles and Thin Films by an Extended RPA. *J. Phys. Metal Phys.*, 4, 1998-2008.
- Crooks, R. M. et al. (2001) Dendrimer-Encapsulated Metal Nanoparticles: Synthesis, Characterization, and Applications to Catalysis. *Acc. Chem. Res.*, 34, 181-190.
- Fu, H. B. and Yao, J. N., Size Effects on the Optical Properties of Organic Nanoparticles. (2001) *J. Am. Chem. Soc.*, 123, 1434-1439.
- Ito, A, et al. (2005) Medical Application of Functionalized Magnetic Nanoparticles. *J. Biosci. Bioeng.*, 100, 1-11.
- Kakuichi, M. et al. (2012) Preparation of Nanoparticles of a Violanthrone Derivative with Properties of J-like Aggregates. *Trans. Mater. Res. Soc. Japan*, 37, 471-474.
- Kasai, H. et al. (1992) A Novel Preparation Method of Organic Microcrystals. *Jpn. J. Appl. Phys.*, 31, L1132-L1134.
- Kasai, H. et al. (1995) Second-Order Hyperpolarizabilities of Aromatic Carboxylates without Visible Absorption. *Jpn. J. Appl. Phys.*, 34, L1208-L1210.
- Kasai, H. et al. (1996) Size-Dependent Colors and Luminescences of Organic Microcrystals, *Jpn. J. Appl. Phys.*, 35, L221-L223.
- Kasatani, K. et al. (2011) Fluorescent Organic Nanoparticles. *Trans. Mater. Res. Soc. Japan*, 36, 421-424.
- Katagi, H. et al. (1996) Size Control of Polydiacetylene Microcrystals. *Jpn. J. Appl. Phys.*, 35, L1364-L1366.
- Kelly, K. L. et al. (2003) Photoinduced Conversion of Silver Nanospheres to Nanoprisms, *J. Phys. Chem. B*, 107, 668-677.

- Mafune, F. et al. (2001) Formation of Gold Nanoparticles by Laser Ablation in Aqueous Solution of Surfactant. *J. Phys. Chem. B*, 105, 5114-5120.
- Takagahara, T. and Takeda. K., (1992) Theory of the Quantum Confinement Effect on Excitons in Quantum Dots of Indirect-gap Materials. *Phys. Rev. B* 46, 15578–15581.
- Tamaki, Y. et al. (2000) Tailoring Nanoparticles of Aromatic and Dye Molecules by Excimer laser Irradiation. *Appl. Surf. Science*, 168, 85-88.
- Tamaki, Y. et al. (2002) Nanoparticle Formation of Vanadyl Phthalocyanine by Laser Ablation of Its Crystalline Powder in a Poor Solvent. *J. Phys. Chem., A*, 106, 2135-2139.
- Tamaki, Y. et al. (2003) Solvent-Dependent Size and Phase of Vanadyl Phthalocyanine Nanoparticles Formed by Laser Ablation of VOPc Crystal-Dispersed Solution. *Jpn. J. Appl. Phys.*, 42, 2725-2729.
- Tan, Z. et al. (2008) Multibranched C₆₀ Micro/Nanocrystals Fabricated by Reprecipitation Method. *Jpn. J. Appl. Phys.*, 47, 1426-1428.
- Tsuji, T. et al. (2001) Preparation of Metal Colloids by Laser Ablation Technique in Solution: Effects of Irradiation Wavelength on the Efficiency of Colloid Formation. *J. Photochem. Photobio. A: Chem.*, 145, 201-207.